Appl. Phys. A 75, 667–672 (2002) / Digital Object Identifier (DOI) 10.1007/s003390201291

Applied Physics A
Materials
Science & Processing

Carbon precipitation and diffusion in SiGeC alloys under silicon self-interstitial injection

D. De Salvador[1,*], **A. Coati**[1], **E. Napolitani**[1], **M. Berti**[1], **A.V. Drigo**[1], **M.S. Carroll**[2,**], **J.C. Sturm**[2], **J. Stangl**[3], **G. Bauer**[3], **L. Lazzarini**[4]

[1] INFM and Dipartimento di Fisica, via Marzolo 8, 35131 Padova, Italy
[2] Department of Electrical Engineering, Princeton University, Princeton, NJ 08544, USA
[3] Institute for Semiconductor Physics, Johannes-Kepler University Linz, Linz, Austria
[4] CNR-MASPEC, Parco Area delle Scienze 37/A, 43010 Fontanini, Parma, Italy

Received: 19 October 2001/Accepted: 19 December 2001/Published online: 20 March 2002 – © Springer-Verlag 2002

Abstract. In this work we investigate the diffusion and precipitation of supersaturated substitutional carbon in 200-nm-thick SiGeC layers buried under a silicon cap layer of 40 nm. The samples were annealed in either inert (N_2) or oxidizing (O_2) ambient at 850 °C for times ranging from 2 to 10 h. The silicon self-interstitial (I) flux coming from the surface under oxidation enhances the C diffusion with respect to the N_2-annealed samples. In the early stages of the oxidation process, the loss of C from the SiGeC layer by diffusion across the layer/cap interface dominates. This phenomenon saturates after an initial period (2–4 h), which depends on the C concentration. This saturation is due to the formation and growth of C-containing precipitates that are promoted by the I injection and act as a sink for mobile C atoms. The influence of carbon concentration on the competition between precipitation and diffusion is discussed.

PACS: 66.30.Jt; 61.72.Cc; 68.35.Dv

1 Introduction

In recent years, strong efforts have been devoted to the investigation of the structural properties of SiGeC alloy, due to its potential use as a Si-based material with band-gap [1] and lattice-parameter [2] tailoring properties. Recently, the role of C in Si and SiGe alloys as a Si self-interstitial (I) trap was evidenced by the reduction of boron equilibrium diffusion [3] and by the suppression of both B transient enhanced diffusion (TED) and B oxidation enhanced diffusion (OED) [4, 5]. This stimulated a renewed interest in the use of SiGeC layers to control the diffusion of dopants in silicon devices.

Therefore, understanding the behavior of C in SiGeC/Si heterostructures under I supersaturation is of crucial importance. It is known that C diffusion is strongly enhanced by I supersaturation [6], as the silicon self-interstitials promote the formation of mobile C interstitial atoms via the kick-out or Frank–Turnbull mechanisms. Recently, a C-diffusion enhancement caused by interstitial injection was also observed in SiGeC alloys with high C concentration, above 10^{20} cm^{-3} [7], leading to a complete loss of C from the alloy. On the other hand, it is well known that C tends to precipitate and to form silicon carbide (SiC) precipitates after thermal annealing in equilibrium conditions [8–11].

The control of the C behavior in Si-based materials under interstitial injection is therefore challenging for technological applications. In this work we report the diffusion and precipitation behavior of C in buried SiGeC layers under supersaturated I non-equilibrium conditions. The non-equilibrium conditions are caused by thermal oxidation of the silicon cap. The concentration profiles of the layer, the strain status of the layer, and the formation of extended defects were monitored as a function of the injected interstitial and for different C concentrations. The distribution of C and the structural transformations were found to depend on a complex competition between C diffusion and C accumulation in precipitates.

2 Experimental

SiGeC layers with a nominal thickness of 200 nm, a Ge concentration of 7 at %, and C concentrations of 0.35 and 0.8 at % have been grown by rapid thermal chemical vapor deposition (RTCVD). The layers were grown over a 200-nm-thick silicon buffer layer at temperatures between 625 °C and 750 °C on a *p*-type Czochralski (100) silicon wafer. A 40-nm-thick Si cap was grown on top of the layers to provide a separation between the SiGeC layers and the surface exposed to O_2 or N_2 during annealing (see below).

The samples were cut into several pieces and thermally treated in a furnace at 850 °C under O_2 or N_2 flux for times ranging from 2 to 10 h. The N_2-annealing experiments were performed in order to distinguish the pure thermal effects from those produced by the I injection under oxidation. According to [11], the SiGeC alloy with a Ge content smaller than 10 at % is relatively stable for a long time (hours)

*Corresponding author.
(Fax: +39-049/827-7003; E-mail: desalvador@padova.infm.it)
***Present address*: Agere Systems, 600 Mountain Avenue, Murray Hill, NJ 07974, USA. (E-mail: malcarroll@agere.com)

under thermal annealing at 850 °C. On the other hand, it is known [12] that at this temperature the I concentration under oxidation is enhanced by about one order of magnitude at the surface, thus providing a large interstitial injection. The I injection into the SiGeC layer strongly depends on the cap-layer thickness; the higher the thickness the lower the interstitial flux into the layer. The 40-nm cap allows a high injection rate [7, 12], allowing at the same time sufficient spatial separation between the SiGeC layer and the growing oxide. In none of the processed samples did oxidation of the SiGeC layer occur: the oxide growth rate was about 0.9 Å/min, not depending on carbon concentration and in good agreement with literature data on dry oxidation of silicon [13]. After annealing under inert (N_2) flux, the oxide thickness was always lower than 2 nm, i.e. comparable to the presence of a native oxide, attesting the absence of significant contamination in the inert atmosphere.

We used Rutherford backscattering spectrometry (RBS) to measure the oxide thickness of the samples, and the thickness of the remaining Si cap after oxidation. The concentration depth profiles of C and Ge were obtained by secondary ion mass spectrometry (SIMS) on a CAMECA IMS-4f spectrometer, using a primary beam of Cs^+ or O_2^+ ions at low impact energies in order to improve the depth resolution. The C and Ge concentrations were calibrated using the total doses obtained by resonant backscattering spectrometry (rBS) and RBS experiments respectively [14], while the depth scale was calibrated by measuring the crater depth with a profilometer. Both cross-sectional and plan-view transmission electron microscopy (TEM) analyses were performed using a JEOL 2000FX microscope operating at 200 kV in order to obtain information on the formation of SiC precipitates within the SiGeC or Si cap layers. High-resolution X-ray diffraction (HRXRD) measurements were performed on a Philips MRD diffractometer equipped with a four-bounce Ge(220) Bartels-type monochromator. (004) rocking curves were recorded using a detector aperture of about 0.5 degrees, from which the strain profile within the SiGeC layer has been obtained, which yields information on the substitutional carbon content.

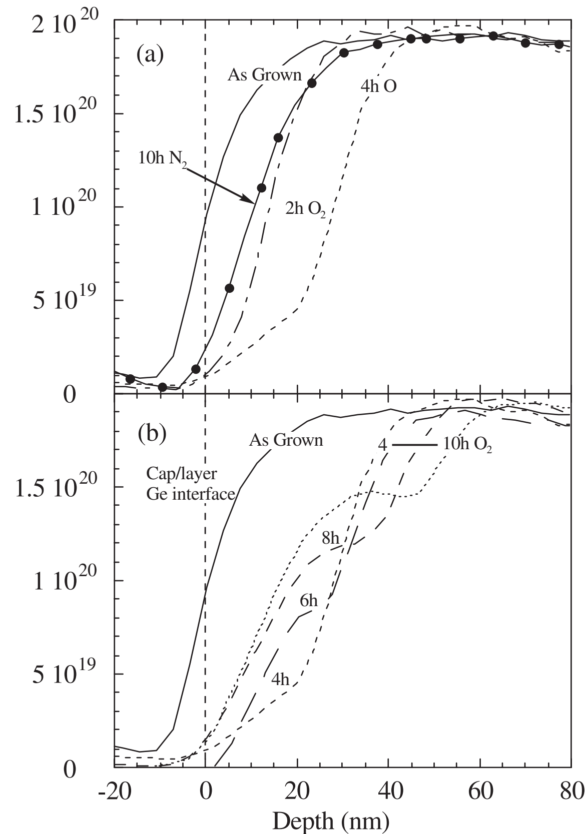

Fig. 1. Carbon concentration profile of the 0.35 at % C samples: (a) as-grown (*continuous line*), 10-h annealed in inert atmosphere (marked by the *arrow*), 2-h (*dot-dashed line*) and 4-h (*dashed line*) oxidation; (b) as-grown (*continuous line*), 4-h, 6-h, 8-h, and 10-h oxidation. All the profiles were shifted in order to have the Ge cap/layer interface at depth zero, marked by the *vertical dashed line*

3 Results

Figure 1 reports the C concentration profiles obtained with SIMS from the samples with the lower (0.35 at %) C content annealed in O_2 and in N_2 at 850 °C. Figure 1a shows a clear non-Fickian diffusion of the C interface closest to the surface. As a matter of fact, no C is detected in the Si cap and no broadening of C profiles is observed, while a shift of the C interface with respect to the Ge interface (vertical dashed line) can be noted. The reason for such a 'non-Fickian' diffusion will be explained in Sect. 4. The figure shows substantially more carbon out-diffusion in the O_2-annealed samples with respect to the N_2-annealed samples, indicating that the I flux enhances the formation of mobile C. As can be noted, the C shift is greater after 2 h of O_2 annealing than after 10 h under inert atmosphere. SIMS analyses showed negligible Ge diffusion in all the processed samples either at the cap/layer or at the layer/substrate interfaces, and no C diffusion occurs in the deeper part of the layer.

The C profile evolution for annealing times longer than 4 h in O_2 (Fig. 1b) shows different features: as the annealing time increases, the interface still moves deeper into the sample but, at the same time, an accumulation kink develops in the region between 20 and 45 nm in depth. Hence, a redistribution of C occurs inside the layer.

Figure 2a reports a cross-sectional TEM image of the 0.35 at % C sample annealed for 8 h in O_2 atmosphere. The formation of defects in the SiGeC layers is clearly visible. Their position coincides with the accumulation kink in the SIMS profile in Fig. 1b. The precipitates have a diameter of about 3–5 nm and are not observed in the N_2-annealed samples even after 10 h of annealing. Cross-sectional TEM images on samples with different O_2-annealing times reveal that the precipitates start to form after 4 h of annealing just below the cap/layer interface. By increasing the annealing time, the precipitates form deeper in the layer, reaching a maximum depth of 120 nm below the SiGeC/Si–cap interface after 10 h. The maximum density of the precipitates occurs at about the same depth where C accumulates according to the SIMS profiles. This correlation between defect formation and the C accumulation suggests that the precipitates contain carbon and that they act as a sink for the mobile C atoms that are produced by the interstitial injection.

By means of plan-view TEM images it was possible to estimate the amount of clusters distributed in the layer. After 10 h of annealing (Fig. 2b) about 8×10^{11} clusters/cm^2 have been formed. By assuming that the precipitates have

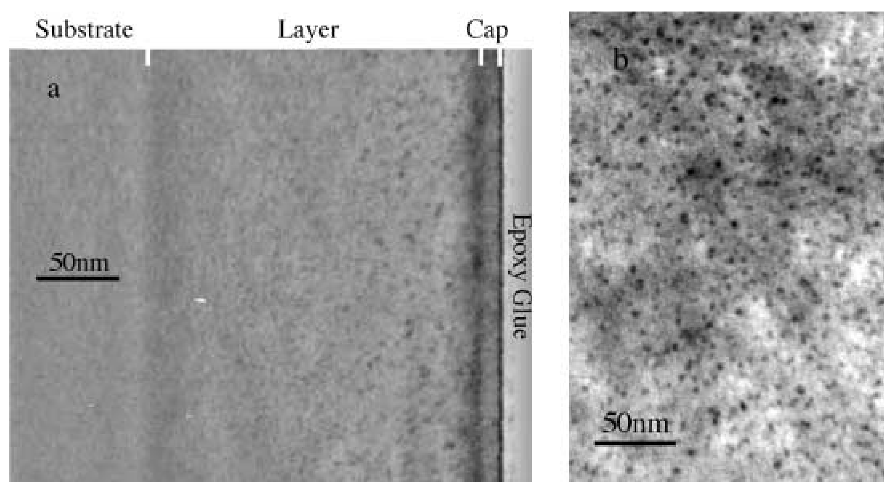

Fig. 2. **a** TEM cross section of the 0.35 at % C sample annealed in O_2 atmosphere for 8 h. Apart from the white glue zone on the right, three zones are visible in the picture. The left-hand zone corresponds to the substrate, the central zone corresponds to the layer, and the right-hand zone is the residual Si cap. The oxide layer is not visible because it was removed by HF etching. The precipitates are distributed inside the layer. **b** Plan-view image of the 0.35 at % sample after 10 h of oxidation

a spherical shape with an average diameter of 4 nm and that they are made of stoichiometric silicon carbide [8–11], the total amount of C in the precipitates is about $(1.3 \pm 0.5) \times 10^{15}$ at/cm^2. If the precipitates were supposed to be formed by graphitic C, the amount of C atoms in the precipitates would turn out to be nearly double and even more in the case of amorphous C.

HRXRD analyses confirm and give further insights into the above process. Figure 3 reports the (004) rocking curve of the sample oxidized for 10 h. Simulation of the rocking curve based on dynamical scattering theory was first attempted by using the C and Ge SIMS profiles (inset of Fig. 3), and considering the Ge and C effects on strain as described in [2]. While this approach provides a successful fit of the as-grown sample rocking curve, in the case of the oxidized sample we found no agreement between the experimental HRXRD data and the dynamical simulation (Fig. 3, dashed line). On the other hand, RBS-channeling experiments show that Ge is still fully on lattice sites even after the longest annealing step. As non-substitutional C incorporated into Si has virtually no influence on the lattice strain [2, 15] and thus has no influence on the HRXRD rocking scans, we conclude that, after annealing in O_2, a certain amount of the carbon detected by SIMS is not on substitutional sites.

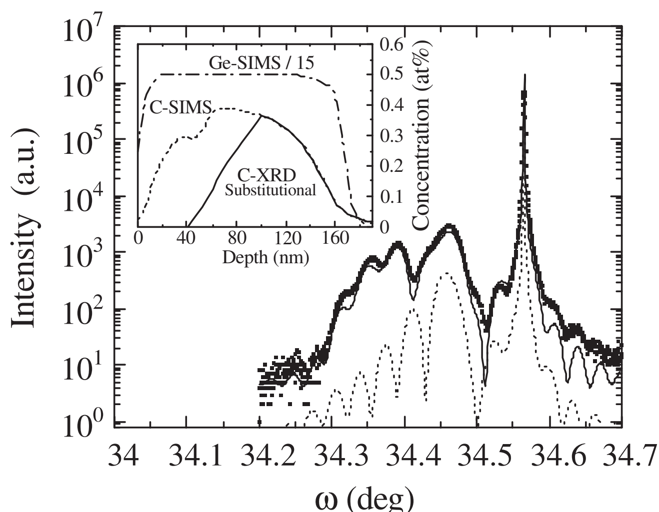

Fig. 3. HRXRD (004) rocking curve of 0.35 at % C, 10-h oxidized sample (*dots*), compared to different simulations. In the *inset*, the concentration profiles used for the simulations are shown. The Ge SIMS profile (*dot-dashed line*) was used for both simulations. The C SIMS profile (*dashed line*) was used to generate the dashed-line simulation, assuming C and Ge to be fully substitutional. The *solid line* is the substitutional C profile used to generate the *continuous-line* rocking curve simulation

Hence, guided by the results shown in Figs. 1 and 2, we assumed that in the first 40 nm of the layer (kink zone) C is fully precipitated, while in the region between 40 and 100 nm its substitutional fraction varies linearly from 0 to 1. That is, we assumed a substitutional C profile as shown by the solid line in the inset of Fig. 3. The good agreement with the experimental data (solid line in Fig. 3) conclusively demonstrates the presence of an extended region of non-substitutional C atoms, which qualitatively follows the precipitate distribution revealed by TEM. Even though we were not able to obtain a direct identification of the precipitate's phase by the TEM experiments, the presence of a silicon carbide phase is suggested by the following compositional analysis. From the difference between the dashed (chemical) and the continuous (substitutional) C profiles of the inset in Fig. 3, it is possible to derive the amount of C atoms on non-substitutional sites. After 10 h of O_2 annealing, this number turns out to be 0.9×10^{15} C atoms/cm^2, which is in good agreement with the amount of C in the precipitates determined by TEM analysis with the assumption of SiC precipitates.

Further insights are given by the experiments on samples with high (0.8 at %) C concentration. Figure 4 reports the evolution, as a function of the oxidation time, of the C profiles in the cap/layer interface region. As can be seen the C loss is stopped after the first 2 h of annealing and nearly no modification is visible during the following annealing steps. In Fig. 5 the amount of C out-diffused through the cap–layer interface is reported for both the C concentrations as a function of the annealing time. As can be noted in both cases the C loss saturates. According to the data in Fig. 5 both the saturation dose and the saturation time appear to decrease by increasing the C concentration.

This fact is related to the earlier precipitate nucleation at higher C content. In fact, TEM analysis of the samples with 0.8 at % C reveals the presence of small precipitates just below the cap/layer interface after 2 h of annealing under oxygen flux (Fig. 6). No evidence of nucleation of such pre-

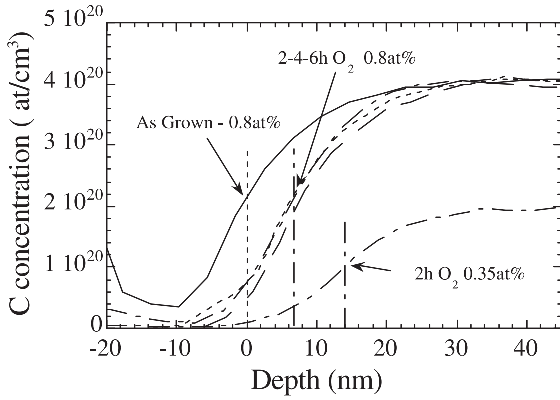

Fig. 4. Carbon concentration profiles of the 0.8 at % C oxidized samples. The as-grown and the 0.35 at % samples oxidized for 2 h are reported for comparison. The *vertical dashed line* represents the initial cap/layer interface, as in Fig. 1, whereas the *dot-dashed lines* mark the profiles' half-height edge

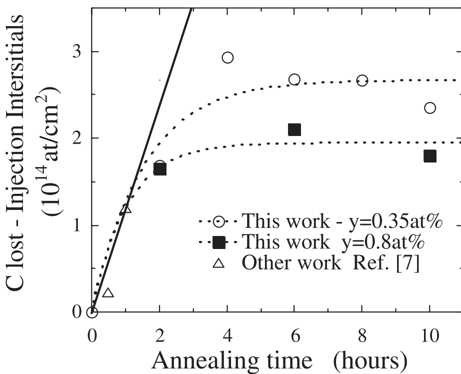

Fig. 5. C dose lost by the layer due to the oxidation process as a function of the annealing time. The C loss is evaluated by calculating the difference between the N_2-annealed and the O_2-annealed C doses. Data of both 0.35 at % C series (*open circles*) and 0.8 at % C series (*full squares*) are reported. *Open triangles* are relative to the data reported in [7] for thin (20 nm) SiGeC layers. The *continuous line* represents the injected I during the thermal oxidation. Exponential fits to the data are reported to guide the eye

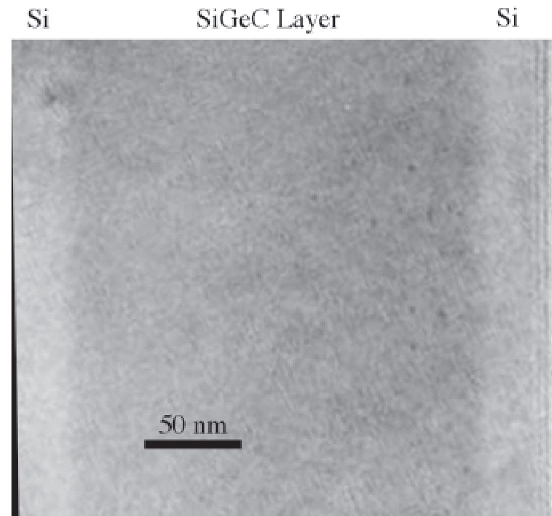

Fig. 6. Cross-sectional TEM image of the 0.8 at % C sample oxidized for 2 h. The presence of small precipitates below the cap–layer interface is visible. Such precipitates are not revealed in the equivalent sample with 0.35 at % C composition

cipitates was found in the sample with 0.35 at % C after the same annealing of 2 h in O_2.

As shown in Fig. 4, no evolution of the C concentration profile is observed for oxidation times longer than 2 h. Nevertheless, the structural properties of the layer change. Indeed, HRXRD reveals that the amount of C in substitutional sites progressively decreases with the oxidation time and that the substitutional C loss goes on progressively from the cap/layer interface to the inner part of the layer.

4 Discussion

Let us start to discuss the low-concentration samples with 0.35 at % C. The surface injection of I produces a significant structural change of the SiGeC layer, starting from the cap/layer interface and proceeding towards higher depths with the annealing time, involving a thickness of about 100 nm after 10 h in O_2. The main physical processes producing this structural modification are caused by C diffusion and precipitation. A schematic explanation of the diffusion–precipitation interplay during the annealing process is proposed in Fig. 7 and discussed below. The basic idea is as follows: interstitials (I) reaching the C interface interact with substitutional C (C_s) to produce a mobile interstitial C (C_i). C_i diffusion leads both to out-diffusion to the surface and to C precipitation in the layer.

Diffusion is clearly enhanced by the I injection, as shown by the differences at the top edge between samples after oxidation or annealing in inert atmosphere. This fact is clearly related to the fact that C diffusion is mediated by Si inter-

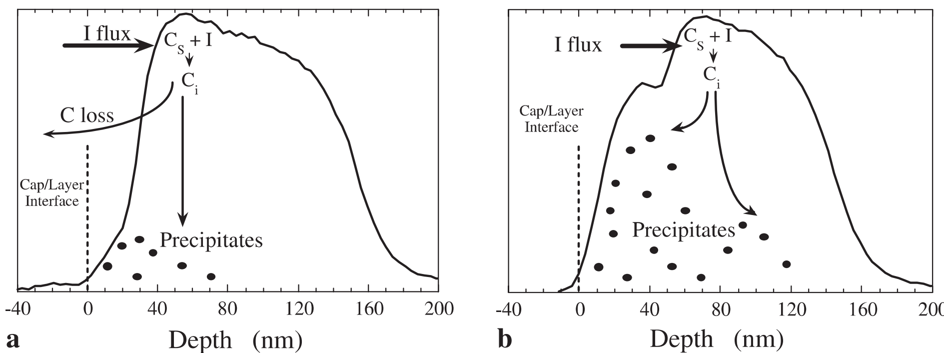

Fig. 7a,b. Schematic view of the diffusion and precipitation interplay under interstitial injection: **a** initial phase of the reaction, I interact with C_s, C_i are formed, the mobile C atoms are lost at the cap/layer interface; **b** second phase, the reaction proceeds, C_s are consumed, C_i are confined in the immobile precipitates, which inhibits further C loss

stitials. The mobile C atoms promoted by the I injection can presumably diffuse both inside the layer and towards the surface. During the first stages of the annealing, C atoms moving towards the surface have an increased mobility, as they are moving inside a region which is rich in I [12]. On the contrary, C atoms moving inside the layer can start nucleating clusters by reacting with other C atoms which in the following could evolve into SiC precipitates. Moreover, following the calculations by Scholz et al. [16], an interstitial undersaturation is produced in the C-rich region and nearly no mobile C is produced inside the layer through the kick-out reaction. As a consequence C atoms at the interface, made mobile by the interaction with I, diffuse out and are not replaced by C atoms diffusing from inside (as would occur in the case of uniform C diffusivity). As a consequence, after 2-h oxidation the net result appears to be a simple shift of the cap/layer C interface instead of a Fickian broadening, thus explaining the diffusion observed in Fig. 1a.

From the data in Fig. 5 it can be deduced that, in the initial stages of the oxidation, the net loss of C atoms from the layer is comparable to the amount of injected interstitials. In fact, the I injection rate, calculated according to [12], turns out to be the same as the initial slope of the C loss. Moreover, SIMS profiles do not show a significant amount of C in the cap; hence the C atoms lost from the layer should be either segregated in the SiO_2 or evaporated at the surface.

After 4-h oxidation, a slight slope change in the bottom part of the C interface shows the formation of the first precipitates. These precipitates are revealed by TEM in the top part of the layer. The growth of the kink from 4 to 10 h of oxidation demonstrates that the precipitates are able to capture mobile C atoms moving towards the surface. The C loss saturates after 4 h, suggesting that at this stage of the process the precipitate's density is sufficiently high to trap the C diffusing atoms with 100% efficiency.

It is interesting to compare the present results with the results relative to thin layers (20 nm) with a similar C composition and a higher Ge content (20 at %) reported in [7]. In that case all carbon in the layer diffuses out after 2 h of interstitial injection leaving no trace of immobile carbon (as measured by SIMS). The precipitation is suppressed in those samples because, presumably, the carbon concentration is depleted by rapid out-diffusion to below a critical density before a significant amount of precipitates can form. As a matter of fact the behavior of the thin samples is perfectly comparable with what happens in the first 20 nm of the layer in the present work, which undergoes a complete C consumption after 2 h of oxidation.

Further information can be obtained by looking at the C redistribution in the layers after the precipitates are nucleated and the C loss reaches saturation. As can be noted in Fig. 1, mobile C atoms are still produced after C-loss saturation, demonstrating that Si interstitials are able to reach the inner part of the layer going through the precipitate area. Therefore it is evident that the precipitates do not act as a sink for Si interstitials (i.e. they trap 100% of C_i but not 100% of I injected). All the mobile C atoms produced between 4 and 10 h of oxidation are captured by the precipitates in the kink of the concentration profile. Following this suggestion the distance between the inner part of the interface where mobile C atoms are produced and the position of the kink gives the order of magnitude of the mobile C atom mean free path in the precipitate-rich zone. This number is about 15 nm.

Following the above scenario, we can easily explain the results of the second set of samples in which the C concentration was raised. The high amount of C increases the precipitation probability as demonstrated in Fig. 6, and therefore the out-diffusion is stopped earlier as shown in Fig. 4. Moreover, the high precipitation probability causes a reduction of the C mean free path or, in other words, it causes a reduction of the distance between the region where mobile C atoms are produced and the region where C capture by precipitates occurs. This reduction is probably the reason why no kink features are revealed in the C profiles of the high-concentration samples (Fig. 4).

The increase of the precipitation probability with increasing concentration ultimately causes a shift in the balance between precipitation and diffusion competition, causing a reduction of the total C loss (Fig. 5). Consequently the C loss reaches saturation in a shorter time and the thickness of the C-depleted zone is reduced (Fig. 4).

5 Conclusions

Clear evidence of a competitive mechanism between C diffusion and precipitation under I injection is reported in this work. In the early stages of oxidation, out-diffusion from the cap/layer dominates, whereas, when precipitation begins to take place, the C loss is progressively suppressed. Precipitates are demonstrated to be fully efficient in trapping the mobile C atoms after an initial transient of C out-diffusion, while they do not trap the Si interstitials. The transient duration and the total amount of C loss depend on the C concentration. Indeed, we have demonstrated that for the higher C concentration, the precipitation probability and efficiency in trapping mobile C atoms are increased. According to the results presented in this work, the balance between C precipitation and diffusion under interstitial injection by oxidation may be controlled by varying the layer thickness and the C concentration.

The dependence of the C loss and precipitation on the layer thickness and composition should be taken into account in the design of Si(Ge)C alloys to be used in microelectronic devices. The general aim of the Si(Ge)C layers is to control the I population and therefore the B anomalous diffusion. On the other hand, the presence of C in an electrically active zone is undesirable because of the deterioration of electrical properties [17, 18]. According to our results, two different approaches could be adopted in order to avoid the contamination of the electrically active layers of the designed structure. If C is originally contained in the electrically active region, the use of thin layers with a low C concentration leads to a complete elimination of C from the designed structure after suitable thermal processes, as demonstrated in [12]. On the contrary, if C is placed outside the electrically active zone, as in [19], the increase of C precipitation by increasing the concentration could contribute to confine C inside the layer and to reduce C diffusion, avoiding contamination of the electrically active zone.

Acknowledgements. The authors wish to thank R. Storti and A. Sambo for technical assistance. This work was partially supported by the SIGENET European Community program, Contract No. HPRN-CT-2000-00123.

References

1. K. Eberl, K. Brunner, O.G. Schmidt: Germanium, Silicon: *Physics and Materials*, ed. by R. Hull, J.C. Bean, Vol. 56 of Semiconductors and Semimetals (Academic, San Diego 1999)
2. D. De Salvador, M. Petrovich, M. Berti, F. Romanato, E. Napolitani, A.V. Drigo, J. Stangl, S. Zerlauth, M. Mühlberger, F. Schäffler, G. Bauer, P.C. Kelires: Phys. Rev. B **61**, 13 005 (2000)
3. H. Rücker, B. Heinemann, W. Röpke, R. Kurps, D. Krüger, G. Lippert, H.J. Osten: Appl. Phys. Lett. **73**, 1682 (1998)
4. P.A. Stolk, D.J. Eaglesham, H.-J. Gossmann, J.M. Poate: Appl. Phys. Lett. **66**, 1370 (1995)
5. M.S. Carroll, C.L. Chang, J.C. Sturm, T. Büyüklimanli: Appl. Phys. Lett. **73**, 3695 (1998)
6. U. Gösele, P. Laveant, R. Scholz, N. Engler, P. Werner: Mater. Res. Soc. Symp. Proc. **610**, B7.1.1 (2000)
7. M.S. Carroll, J.C. Sturm, D. De Salvador, E. Napolitani, M. Berti, J. Stangl, G. Bauer: Phys. Rev. B **64**, 073308 (2001)
8. J.W. Strane, H.J. Stein, S.R. Lee, S.T. Picraux, J.K. Watanabe, J.W. Mayer: J. Appl. Phys. **76**, 3656 (1994)
9. A.R. Powell, F.K. LeGoues, S.S. Iyer: Appl. Phys. Lett. **64**, 324 (1994)
10. G.G. Fischer, P. Zaumseil, E. Bugiel, H.J. Osten: J. Appl. Phys. **77**, 1934 (1995)
11. L.V. Kulik, D.A. Hits, M.W. Dashiell, J. Kolodzey: Appl. Phys. Lett. **72**, 1972 (1998)
12. M.S. Carroll, J.C. Sturm, T. Büyüklimanli: Phys. Rev. B **64**, 085316 (2001)
13. D. Skarlatos, M. Omri, A. Claverie, D. Tsoukalas: J. Electrochem. Soc. **146**, 2276 (1999)
14. M. Berti, D. De Salvador, A.V. Drigo, F. Romanato, A. Sambo, S. Zerlauth, J. Stangl, F. Schäffler, G. Bauer: Nucl. Instrum. Methods B **143**, 357 (1998)
15. J. Tersoff: Phys. Rev. Lett. **64**, 1757 (1990)
16. R. Scholz, U. Gösele, J.-Y. Huh, T.Y. Tan: Appl. Phys. Lett. **72**, 200 (1998)
17. F. Priolo, G. Mannino, M. Miccichè, V. Privitera, E. Napolitani, A. Carnera: Appl. Phys. Lett. **72**, 3011 (1998)
18. H.J. Osten, G. Lippert, P. Gaworezewski, R. Sorge: Appl. Phys. Lett. **71**, 1522 (1997)
19. E. Napolitani, A. Coati, D. De Salvador, A. Carnera, S. Mirabella, S. Scalese, F. Priolo: Appl. Phys. Lett. **79**, 4145 (2001)